Modal spectrum in spontaneous parametric down-conversion with noncollinear phase matching

Yingwen Zhang and Filippus S. Roux
CSIR National Laser Centre, P. O. Box 395, Pretoria 0001, South Africa
(Received 28 March 2014; published 5 June 2014)

We investigate the effect of the down-conversion angle between the signal and idler beams in spontaneous parametric down-conversion on the bandwidth of the modal spectrum (Schmidt number) of the down-converted quantum state. For this purpose, we consider both the full Schmidt number and the azimuthal Schmidt number in the Laguerre-Gaussian basis. For the full Schmidt number, we show that the approximation of the phase-matching function with a Gaussian function gives results that disagree significantly from those obtained with the more physical sinc-type phase-matching function. We found a drastic increase in both the Schmidt number and the azimuthal Schmidt number for small down-conversion angles, in agreement with recent experimental results.

DOI: 10.1103/PhysRevA.89.063802 PACS number(s): 42.65.Lm, 42.50.Dv, 42.50.Tx, 03.67.Bg

I. INTRODUCTION

Entanglement of photonic states is one of the central concepts in quantum information and quantum optics. A proper understanding and use of entanglement can lead to significant technological advances in communication, computing, and cryptography [1]. Pairs of entangled photons are readily produced through spontaneous parametric down-conversion (SPDC) [2–4]. Down-converted photons can be entangled in a wide variety of forms, including polarization, temporal frequencies [5,6], energy-time variables [7,8], and orbital angular momentum (OAM) [9–11]. These forms of entangled photons have been used to test the violation of Bell's inequality [12], to demonstrate quantum teleportation [13,14], and to realize quantum communication [15].

The degree of entanglement of a quantum state can be quantified by the Schmidt number [16,17]. A large Schmidt number indicates a large degree of entanglement in the biphoton state, thus allowing more quantum information to be encoded. When restricted to the OAM degrees of freedom in a Laguerre-Gaussian (LG) basis (by fixing the radial degrees of freedom), the equivalent quantity is called the azimuthal Schmidt number. One can use the azimuthal Schmidt number to quantify the width of the OAM spectrum, the spiral bandwidth [17–21].

By manipulating the experimental parameters of the SPDC setup, one can increase the spiral bandwidth. However, this is usually done while maintaining collinear phase matching, i.e., with collinear signal and idler beams [20–23]. Recently, Romero *et al.* [24] considered the effect of a small down-conversion angle and found a drastic increase in the spiral bandwidth. Apart from an insightful qualitative explanation involving the étendue [24], the reason for this drastic increase is not well understood.

In this paper, we provide a theoretical analysis of the effect of a noncollinear down-conversion angle on the full Schmidt number and the azimuthal Schmidt number. The full Schmidt number for noncollinear down-conversion can be calculated analytically by approximating the phase-matching function by a Gaussian function, as was done previously [17]. However, comparing this result to a result that employs the more physical sinc-type phase-matching function, one finds that there is a significant difference. The Gaussian approximation only gives a small change in the Schmidt number for small down-conversion angles, whereas the case with the sinc function produces a drastic increase in the Schmidt number.

Next, we investigate the effect of the down-conversion angle on the azimuthal Schmidt number in the LG basis. For this purpose we use generating functions for the LG modes and are therefore able to obtain analytical results, provided that we assume that the nonlinear crystal length is much shorter than the Rayleigh range of the pump beam. From these expressions we are able to show that the azimuthal Schmidt number increases drastically for small down-conversion angles, consistent with the drastic increase seen in the full Schmidt number.

II. THEORETICAL BACKGROUND

The probability amplitude for a pump photon to be converted into a pair of down-converted photons through the SPDC process, with degenerate type I phase matching, can be expressed as

$$\mathcal{M} = \Omega_0 \int M_s^*(\mathbf{q}_s) M_i^*(\mathbf{q}_i) M_p(\mathbf{q}_p) \times \delta(\Delta\mathbf{q}) S(\Delta k_z) \frac{d^2q_s}{(2\pi)^2} \frac{d^2q_i}{(2\pi)^2} \frac{d^2q_p}{(2\pi)^2}, \quad (1)$$

where Ω_0 is the overall conversion efficiency and $\mathbf{q}$ and k_z are, respectively, the transverse and longitudinal components of the wave vector $\mathbf{k}$. The angular spectra of the beam profiles are given by $M_s(\mathbf{q})$, $M_i(\mathbf{q})$, and $M_p(\mathbf{q})$ for the signal, idler, and pump beams, respectively. The phase-matching function $S(\Delta k_z)$ is given by [25]

$$S(\Delta k_z) = \mathrm{sinc}\left(\frac{\Delta k_z L}{2}\right), \quad (2)$$

where L is the thickness of the nonlinear crystal in the longitudinal direction and

$$\Delta k_z = n_p k_{p,z} - n_s k_{s,z} - n_i k_{i,z}, \quad (3)$$

with n_x being the refraction index, as applicable for the different beams. The argument of the Dirac delta function $\delta(\Delta\mathbf{q})$ is

$$\Delta\mathbf{q} = n_p\mathbf{q}_p - n_s\mathbf{q}_s - n_i\mathbf{q}_i. \quad (4)$$

For type I phase matching, we have $n_s = n_i = n_o$, where n_o is the ordinary refractive index.

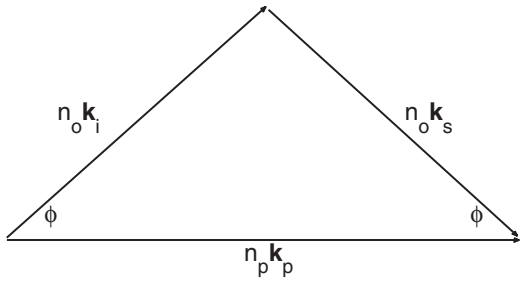

FIG. 1. Vector diagram showing condition for perfect phase matching.

In the degenerate case, we have $|\mathbf{k}_\mathrm{s}| = |\mathbf{k}_\mathrm{i}| = \omega_p/2c$, where ω_p is the angular frequency of the pump. Hence, due to the conservation of energy, $|\mathbf{k}_\mathrm{p}| = |\mathbf{k}_\mathrm{s}| + |\mathbf{k}_\mathrm{i}| = \omega_p/c$. From Fig. 1 we see that for perfect phase matching

$$n_\mathrm{p} = n_\mathrm{o}\cos(\phi), \tag{5}$$

where ϕ is the down-conversion angle, i.e., the angle between the propagation vector of the pump beam and that of either the signal or idler beams. If $\phi \neq 0$, Eq. (3) can be written as

$$\Delta k_z = n_\mathrm{o}[\cos(\phi)k_{z\mathrm{p}} - k_{z\mathrm{s}} - k_{z\mathrm{i}}], \tag{6}$$

and $\delta(\Delta\mathbf{q})$ then implies that one can substitute

$$\mathbf{q}_\mathrm{p} = \frac{\mathbf{q}_\mathrm{s} + \mathbf{q}_\mathrm{i}}{\cos(\phi)}. \tag{7}$$

In the paraxial limit, it can be shown that (see the Appendix)

$$\Delta k_z = n_\mathrm{o}\left[\frac{\lambda_\mathrm{p}|\mathbf{q}_\mathrm{i} - \mathbf{q}_\mathrm{s}|^2}{4\pi\cos(\phi)} - \frac{\pi\sin^2(\phi)}{\lambda_\mathrm{p}\cos(\phi)}\right]. \tag{8}$$

To simplify notation we will use normalized (dimensionless) spatial frequencies

$$\mathbf{q} = \frac{2\pi\mathbf{a}}{w_\mathrm{p}}, \tag{9}$$

where w_p is the radius of the pump beam.

Being a Gaussian beam, the pump beam's angular spectrum is expressed as

$$M_\mathrm{p} = \exp\left[\frac{-\pi^2|\mathbf{a}_\mathrm{s} + \mathbf{a}_\mathrm{i}|^2}{\cos^2(\phi)}\right], \tag{10}$$

and the phase-matching function is given by

$$S(\Delta k_z) = \mathrm{sinc}\left[\frac{\pi^2\beta|\mathbf{a}_\mathrm{s} - \mathbf{a}_\mathrm{i}|^2}{2\cos(\phi)} - \frac{\chi}{2}\right], \tag{11}$$

where

$$\chi = \frac{\pi n_\mathrm{o} L\sin^2(\phi)}{\lambda_\mathrm{p}\cos(\phi)} \tag{12}$$

and

$$\beta = \frac{n_\mathrm{o}L\lambda_\mathrm{p}}{\pi w_\mathrm{p}^2} = \frac{n_\mathrm{o}L}{z_R}, \tag{13}$$

with z_R being the Rayleigh range.

Writing Eq. (1) in terms of the normalized frequencies and evaluating the a_p^2 integral, we obtain

$$\mathcal{M} = \tilde{\Omega}_0 \int \tilde{M}_\mathrm{s}^*(\mathbf{a}_\mathrm{s})\tilde{M}_\mathrm{i}^*(\mathbf{a}_\mathrm{i})\exp\left[\frac{-\pi^2|\mathbf{a}_\mathrm{s} + \mathbf{a}_\mathrm{i}|^2}{\cos^2(\phi)}\right] \times \mathrm{sinc}\left[\frac{\pi^2\beta|\mathbf{a}_\mathrm{s} - \mathbf{a}_\mathrm{i}|^2}{2\cos(\phi)} - \frac{\chi}{2}\right] d^2a_\mathrm{s}d^2a_\mathrm{i}, \tag{14}$$

where $\tilde{\Omega}_0 = \Omega_0 w_\mathrm{p}^6$ and $\tilde{M}_{\mathrm{s,i}}(\mathbf{a}_{\mathrm{s,i}}) = M_{\mathrm{s,i}}(2\pi\mathbf{a}_{\mathrm{s,i}}/w_\mathrm{p})$.

III. FULL SCHMIDT NUMBER

Here we will compute the Schmidt number for the down-converted state $|\Psi\rangle$ after SPDC. This state is given by the product of the pump beam and the phase-matching function, as given in Eqs. (10) and (11). Hence,

$$\Psi(\mathbf{a}_\mathrm{s},\mathbf{a}_\mathrm{i}) = \langle\mathbf{a}_\mathrm{s},\mathbf{a}_\mathrm{i}|\Psi\rangle = \mathcal{N}S(\Delta k_z)M_\mathrm{p}(\mathbf{a}_\mathrm{s},\mathbf{a}_\mathrm{i}), \tag{15}$$

where $\mathcal{N}$ is a normalization constant that ensures

$$\int |\Psi(\mathbf{a}_\mathrm{s},\mathbf{a}_\mathrm{i})|^2\, d^2a_\mathrm{s}d^2a_\mathrm{i} = 1. \tag{16}$$

The Schmidt decomposition of a bipartite pure state is given by

$$|\Psi\rangle = \sum_n c_n\,|\Phi_n\rangle_\mathrm{A}\,|\Phi_n\rangle_\mathrm{B}\,, \tag{17}$$

where c_n denotes the Schmidt coefficients and $|\Phi_n\rangle_\mathrm{A}$ and $|\Phi_n\rangle_\mathrm{B}$ are the Schmidt bases in the respective subsystems. The normalization of the pure state requires that $\sum_n c_n^2 = 1$. The (full) Schmidt number of this state is given by

$$K = \frac{1}{\sum c_n^4} = \frac{1}{\mathrm{tr}\{\rho_A^2\}}, \tag{18}$$

where ρ_A is the reduced density matrix of the state.

A. Gaussian approximation

First, we use the approach of Law and Eberly [17] to estimate the Schmidt number. In this approach the phase-matching function is approximated by a Gaussian function. Hence, the down-converted state is given by[1]

$$\Psi_g(\mathbf{a}_\mathrm{s},\mathbf{a}_\mathrm{i}) = \mathcal{N}_g\exp\left[\frac{-\pi^2|\mathbf{a}_\mathrm{s} + \mathbf{a}_\mathrm{i}|^2}{\cos^2(\phi)}\right]\exp\left[-\frac{\pi^2\beta|\mathbf{a}_\mathrm{s} - \mathbf{a}_\mathrm{i}|^2}{2\cos(\phi)}\right]. \tag{19}$$

Using the normalization condition in Eq. (16), we calculate the normalization constant to be

$$|\mathcal{N}_g|^2 = \frac{8\pi^2\beta}{\cos^3(\phi)}. \tag{20}$$

The reduced density matrix ρ_A in Eq. (18) can be computed by

$$\rho_A(\mathbf{a}_\mathrm{s},\mathbf{a}_\mathrm{s}') = \int \Psi_g(\mathbf{a}_\mathrm{s},\mathbf{a}_\mathrm{i})\Psi_g^*(\mathbf{a}_\mathrm{s}',\mathbf{a}_\mathrm{i})\, d^2a_\mathrm{i}. \tag{21}$$

[1]We neglect the second term in the argument of Eq. (11) because, being independent of the spatial frequencies, it is removed through normalization.

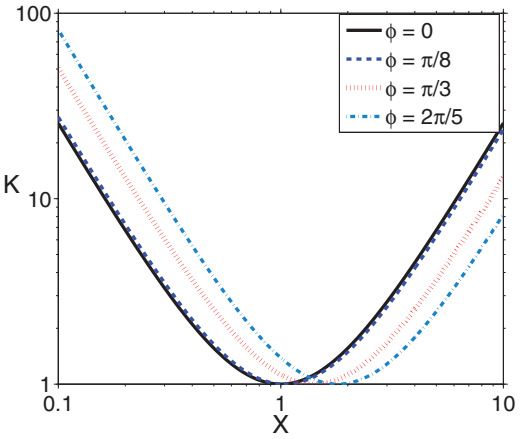

FIG. 2. (Color online) Plot of the Schmidt number K as a function of X on a logarithmic scale for various down-conversion angles, using a Gaussian approximation for the phase-matching function.

The trace of the square of the reduced density matrix is given by

$$\mathrm{tr}\{\rho_A^2\} = \int \rho_A(\mathbf{a}_s,\mathbf{a}_s')\rho_A(\mathbf{a}_s',\mathbf{a}_s)\, d^2a_s\, d^2a_s'. \tag{22}$$

After evaluation of these integrals, we obtain

$$K = \frac{1}{4}\left(\frac{1}{X\sqrt{\cos(\phi)}} + X\sqrt{\cos(\phi)}\right)^2, \tag{23}$$

where $X = \sqrt{\beta/2}$. Hence, K depends only on β and the down-conversion angle ϕ. For $\phi = 0$, the expression becomes equal to the one in [17].

In Fig. 2 we plot K as a function of X on a log-log plot for various down-conversion angles, as expressed in Eq. (23). Since $\cos(\phi)$ acts as a scale factor for X in Eq. (23), a change in the angle ϕ produces a horizontal shift of the curve on the logarithmic axis. As a result, K only increases for $X < 1$. Since most experimental setups are such that $X \ll 1$, one would, in general, observe an increase in K. However, we see in Fig. 2 that the change in K is negligible for small ϕ; for instance, even when $\phi = \pi/8$, the change is still barely noticeable.

From the above discussion we conclude that the calculation of the Schmidt number using the Gaussian approximation does not explain the drastic increase in the spiral bandwidth that was observed in [24]. For this reason we now turn our attention to the calculation of the Schmidt number using the sinc-type phase-matching function, i.e., without the Gaussian approximation.

B. Sinc-type phase-matching function

Using the sinc-type phase-matching function, we obtain the following expression for the down-converted state:

$$\Psi_s(\mathbf{a}_s,\mathbf{a}_i) = \mathcal{N}_s \exp\left[\frac{-\pi^2|\mathbf{a}_s+\mathbf{a}_i|^2}{\cos^2(\phi)}\right] \times \mathrm{sinc}\left[\frac{\pi^2\beta|\mathbf{a}_s-\mathbf{a}_i|^2}{2\cos(\phi)} - \frac{\chi}{2}\right]. \tag{24}$$

The normalization constant $\mathcal{N}_s$, computed with the aid of Eq. (16), is given by

$$|\mathcal{N}_s|^2 = \frac{8\pi^2\beta\chi}{\cos^3(\phi)[-2-\pi\chi+2\mathrm{Si}(\chi)\chi+2\cos(\chi)]}, \tag{25}$$

where $\mathrm{Si}(\cdot)$ is the sine integral function and χ is given in Eq. (12). In the limit where $\phi \to 0$, we have $|N_s|^2 \to 8\pi^2\beta$.

To simplify the integrations, we rewrite the sinc function as

$$\mathrm{sinc}(x) = \frac{1}{2}\int_{-1}^{1} \exp(-ixt)\, dt. \tag{26}$$

Using Eqs. (26), (21), and (22), we obtain

$$\mathrm{tr}\{\rho_A^2\} = \frac{2\beta\chi^2\cos(\phi)}{[2\mathrm{Si}(\chi)\chi-\pi\chi+2\cos(\chi)-2]^2} \times \iiiint_{-1}^{1} \mathcal{T}\, dt_1\, dt_2\, dt_3\, dt_4, \tag{27}$$

where

$$\mathcal{T} = \exp\left[-\frac{i\chi}{2}(t_1-t_2+t_3-t_4)\right] \times \{i\beta^2\cos^2(\phi)[(t_1+t_3)t_2t_4-(t_2+t_4)t_1t_3] + 2\beta\cos(\phi)[(t_1+t_3)(t_2+t_4)-2(t_1t_3+t_2t_4)] - i4(t_1-t_2+t_3-t_4)\}^{-1}. \tag{28}$$

Unfortunately, the integrals over the auxiliary variables t_1, t_2, t_3, and t_4 in Eq. (27) are not tractable. Nevertheless, one can obtain an analytical solution if one exploits a condition that is applicable in typical experimental setups, namely, $L \ll z_R$. This condition, which we call the thin-crystal limit, implies that $\beta \ll 1$. Therefore, one can expand the expressions in Eq. (28) to leading order in β.[2] After evaluating the integrals, the result is

$$\mathrm{tr}\{\rho_A^2\} = \frac{-8\beta\cos(\phi)}{3[2\mathrm{Si}(\chi)\chi-\pi\chi+2\cos(\chi)-2]^2\chi} \times \{\chi^3[2\mathrm{Si}(\chi)-4\mathrm{Si}(2\chi)+\pi] + 2[1-\cos(\chi)+\chi\sin(\chi)]^2 - 2[1-\cos(\chi)][\sin(\chi)-\chi\cos(\chi)]\chi\}. \tag{29}$$

Although we made the expansion in β, Eq. (29) is only valid for $\phi \lesssim 0.01$ rad. The reason is that λ_p is, in general, small ($\sim$1 μm); as a result χ can be quite large when ϕ is not small.

In Fig. 3, we compare the curve for Eq. (29) to a numerical estimate of K as a function of ϕ. For the numerical estimate of K we performed a Monte Carlo integration of Eq. (27). The experimental parameters for these curves are $L = 5$ mm, $w_p = 1$ mm, $\lambda_p = 0.355$ μm and $n_o = 1.7$, which gives $\beta \approx 1 \times 10^{-3}$. One can see that K increases rapidly up to an angle of approximately $\phi = 0.01$ rad, where it reaches a value of about double the value at $\phi = 0$. Up to this point the theoretical curve and the numerical results are in good agreement. Beyond this point these curves start to diverge. Note that the point

[2]This implies that we set $\beta = 0$ in $\mathcal{T}$.

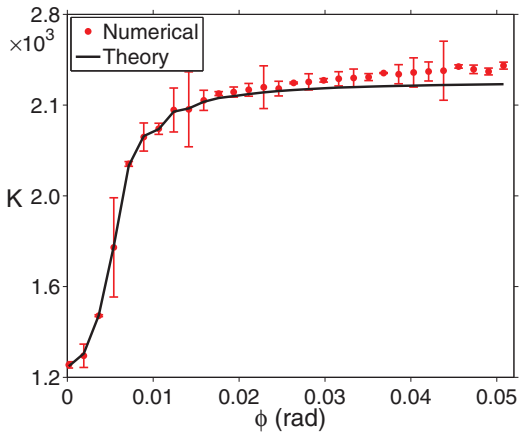

FIG. 3. (Color online) The Schmidt number as a function of the down-conversion angle. The solid line is the theoretical curve in the small-crystal limit [Eq. (29)]. The data points give the general solution obtained numerically with the aid of Monte Carlo integration of Eq. (27). The error bars represent the standard deviation.

where $\phi = 0.01$ rad is where $\chi \approx \pi$, which may explain the qualitative change in the curve in Fig. 3 at this point.

Comparing the angular dependence of K with and without the Gaussian approximation, shown in Figs. 2 and 3, respectively, we notice a significant difference. For the Gaussian approximation, when using Eq. (23) with the above parameters, we obtain $K = 521$ and K is essentially constant in the angular region plotted in Fig. 3; however, the increase in K when considering it without the Gaussian approximation is much more drastic. As a result, we conclude that the Gaussian approximation of the phase-matching function does not give reliable results under noncollinear phase-matching conditions.

IV. AZIMUTHAL SCHMIDT NUMBER

The increase in the (full) Schmidt number for small down-conversion angles indicates what happens to the modal content of the full down-converted quantum state. The question remains, what happens to the modal spectrum that is measured? Such a measurement depends on the measurement setup. In the case where one is interested in the OAM spectrum, the radial dependence of the modes is fixed in some way by the experimental setup. The azimuthal Schmidt number depends on the shape of the radial dependence of the OAM modes, as determined by the experiment setup. Often the OAM modes are specified as helical phase functions on the spatial light modulators that are used to modulate the signal and idler beams. In such a case the radial mode profiles of all modes, regardless of OAM, are close to a Gaussian function. Such modes can be referred to as helical Gaussian modes. However, low-pass spatial filtering imposed by the limiting aperture in the optical system can convert the helical Gaussian modes into modes that more closely resemble Laguerre-Gaussian modes with a zero radial index $p = 0$.

To allow for this variability, we start by calculating the OAM spectrum in the Laguerre-Gaussian basis for arbitrary azimuthal and radial indices. This is done by leaving the p dependence implicit in terms of generating parameters. Eventually, we set the radial index to zero $p = 0$ for both beams when we calculate the azimuthal Schmidt number for quantitative comparison.

The azimuthal Schmidt number is given by

$$\kappa = \frac{1}{\sum_\ell P_\ell^2}, \tag{30}$$

where ℓ is the azimuthal index, which is proportional to the OAM of the modes, and $P_\ell(\propto|\mathcal{M}|^2)$ represents the probability to observe a particular pair of OAM modes with a fixed radial dependence.

For the calculation of the OAM spectrum with Eq. (1), we will use a generating function for the angular spectra of LG modes to represent the signal and idler beams. This generating function is given by [26]

$$\mathcal{G} = \frac{1}{1+\eta}\exp\left[\frac{i(q_x \pm iq_y)w\mu}{2(1+\eta)} - \frac{(q_x^2+q_y^2)w^2(1-\eta)}{4(1+\eta)}\right], \tag{31}$$

where w is the radius of the beam waists and the sign in the exponent is given by the sign of ℓ. The angular spectra of the signal and idler beam profiles for particular LG modes are obtained by

$$M_{\mathrm{s,i}}^{\ell,p}(\mathbf{q}) = \mathcal{N}_{\mathrm{LG}}\frac{1}{p!}\left[\partial_\eta^p \partial_\mu^{|\ell|}\mathcal{G}\right]_{\eta,\mu=0}, \tag{32}$$

where μ and η are generating parameters for the azimuthal and radial indices, respectively, and

$$\mathcal{N}_{\mathrm{LG}} = \left[\frac{2\pi 2^{|\ell|}p!}{(p+|\ell|)!}\right]^{1/2}. \tag{33}$$

It is assumed that the radii of the beam waists of the signal and idler beams are equal, $w_\mathrm{s} = w_\mathrm{i} = w$.

We evaluate the overlap integral equation (14), with the signal and idler modes given by Eq. (31). The integral is zero, unless the azimuthal indices of the signal and idler beams have opposite signs and equal magnitudes. Hence, we evaluate the expression for explicit azimuthal indices given by $\ell_\mathrm{s} = -\ell_\mathrm{i} = \ell$. The radial indices of the signal and idler beams are left implicit in terms of the generating parameters η_s and η_i, respectively. Using Eq. (26) to rewrite the sinc function and integrating over $\mathbf{q}_\mathrm{s}$ and $\mathbf{q}_\mathrm{i}$, we obtain

$$\mathcal{G}_\ell = \alpha\cos^3(\phi)\int_{-1}^{1}\exp\left(\frac{-i\chi t}{2}\right) \times \frac{\left\{\alpha\cos(\phi)\left[1+\frac{i}{2}\beta\cos(\phi)t\right]\right\}^{|\ell|}}{[\alpha\cos(\phi)\mathcal{A} - i\beta\mathcal{B}t]^{1+|\ell|}}dt, \tag{34}$$

which is a generating function for $\mathcal{M}$, where β and χ are given in Eqs. (13) and (12), respectively, and

$$\alpha = \frac{w^2}{w_p^2}, \tag{35}$$

$$\mathcal{A} = \alpha\cos^2(\phi)(1-\eta_\mathrm{s})(1-\eta_\mathrm{i}) + 2(1-\eta_\mathrm{s}\eta_\mathrm{i}), \tag{36}$$

$$\mathcal{B} = \alpha\cos^2(\phi)(1-\eta_\mathrm{s}\eta_\mathrm{i}) + 2(1+\eta_\mathrm{s})(1+\eta_\mathrm{i}). \tag{37}$$

To obtain the probability amplitude for particular radial indices p and q of the signal and idler beams, respectively,

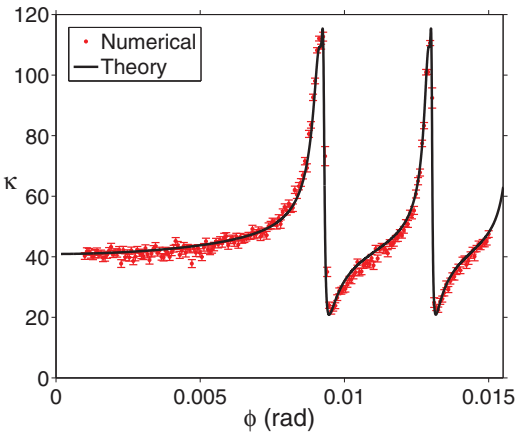

FIG. 4. (Color online) The azimuthal Schmidt number κ as a function of ϕ for the case $p = q = 0$ and $\alpha = 0.1$. The solid black curve is the theoretically determined result in the small-β limit using Eq. (40). The red points are the numerical results from Eq. (14) determined using the Monte Carlo integration method, with error bars indicating the standard deviation.

one evaluates the following operation:

$$\mathcal{M} = \frac{\Omega_0}{w_p}\mathcal{N}_{pq}\left[\partial_{\eta_s}^p \partial_{\eta_i}^q \mathcal{G}_\ell\right]_{\eta_s,\eta_i=0}, \tag{38}$$

where

$$\mathcal{N}_{pq} = \frac{2^{(|\ell|+1/2)}|\ell|!}{[\pi(p+|\ell|)!(q+|\ell|)!p!q!]^{1/2}}. \tag{39}$$

We apply the thin-crystal approximation and expand the integrand in Eq. (34) to next-to-leading order in β. The result can then be integrated to give

$$\begin{aligned}\mathcal{G}_\ell = {} & \frac{4\cos^2(\phi)}{\chi\mathcal{A}^{1+|\ell|}}\sin\left(\frac{\chi}{2}\right) \\ & - \frac{2\beta\cos(\phi)[\alpha\cos^2(\phi)|\ell|\mathcal{A} + 2(1+|\ell|)\mathcal{B}]}{\alpha\chi^2\mathcal{A}^{2+|\ell|}} \\ & \times\left[\cos\left(\frac{\chi}{2}\right)\chi - 2\sin\left(\frac{\chi}{2}\right)\right].\end{aligned} \tag{40}$$

Figure 4 shows the theoretical and numerical curve of the azimuthal Schmidt number κ with $p = q = 0$ and $\alpha = 0.1$ as a function of ϕ. The theoretical curve is given by Eq. (40), and the numerical curve is obtained from a numerical evaluation of Eq. (14), using Monte Carlo integration. The experimental parameters for the curve are $L = 5$ mm, $w_p = 1$ mm, $\lambda_p = 0.355$ μm, and $n_o = 1.7$. One can see in Fig. 4 that κ increases rapidly as it approaches the point where $\phi \approx 0.009$ rad, reaching a maximum of approximately 3 times the value at $\phi = 0$ before suddenly decreasing to a minimum of around half the value at $\phi = 0$. We find that κ oscillates between maxima and minima that slowly increase with ϕ. However, the gradual change in the maxima and minima in κ is only noticeable when $\phi > 0.2$ rad. The oscillating frequency also increases with ϕ.

We see the same oscillatory behavior in Fig. 5, where we plotted κ as a function of ϕ for the case $p = 3$, $q = 1$ with $\alpha = 0.1$ using the same experimental parameters. It is

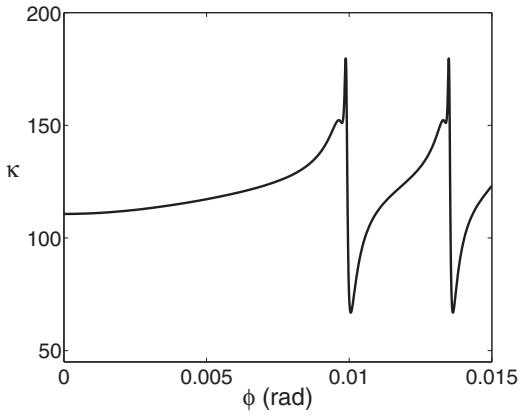

FIG. 5. The azimuthal Schmidt number κ as a function of ϕ for the case $p = 3$, $q = 1$, and $\alpha = 0.1$.

as expected that a larger κ is obtained at $\phi = 0$; however, the maximum reached is now only about 1.5 times the value at $\phi = 0$, and the first maximum is shifted to a larger value of ϕ ($\phi \approx 0.0098$ rad). We found that when larger values of p and q are used and also when $|p - q|$ increases, the ratio between the first maximum of κ and that at $\phi = 0$ decreases, and the maximum shifts to increasingly larger values of ϕ. If one is to compute the full Schmidt number as a function of ϕ, we expect that these oscillations will be smeared out by the shifted maxima and minima of larger radial modes, eventually reproducing the curve seen in Fig. 3.

The widths of the peaks in κ as a function of ϕ are determined by the value of α. To demonstrate this we show in Fig. 6 the azimuthal Schmidt number as a function of ϕ for $\alpha = 0.5$. The azimuthal Schmidt number shows the same oscillatory behavior as for $\alpha = 0.1$, but the peaks are much narrower. Note that in Fig. 6(a), the value of κ seems to diverge at $\phi \approx 0.009$ rad, but that is not the case. An expanded view of the region near $\phi = 0.009$ rad is shown in Fig. 6(b). One can see that κ merely changes very rapidly.

V. CONCLUSION

The effect of the down-conversion angle between the signal and idler beams on the modal spectrum of the down-converted state is studied. The Schmidt number, which quantifies the effective number of entangled modes in the down-converted state, is shown to increase drastically for small down-conversion angles, as was observed in a recent experiment [24]. Due to this increase, the Schmidt number can be as large as double the nominal value at collinear down-conversion. To show this increase analytically, one needs to consider the physical sinc-function phase-matching condition since the Gaussian approximation does not provide accurate results for nonzero down-conversion angles. We made the assumption that the length of the nonlinear crystal is much shorter than the Rayleigh range of the pump beam, i.e., the thin-crystal approximation, which is true in most practical down-conversion experiments.

The modal spectrum that is measured in a physical experiment depends on the modal basis in terms of which the measurements are made. Often an OAM basis is used, such

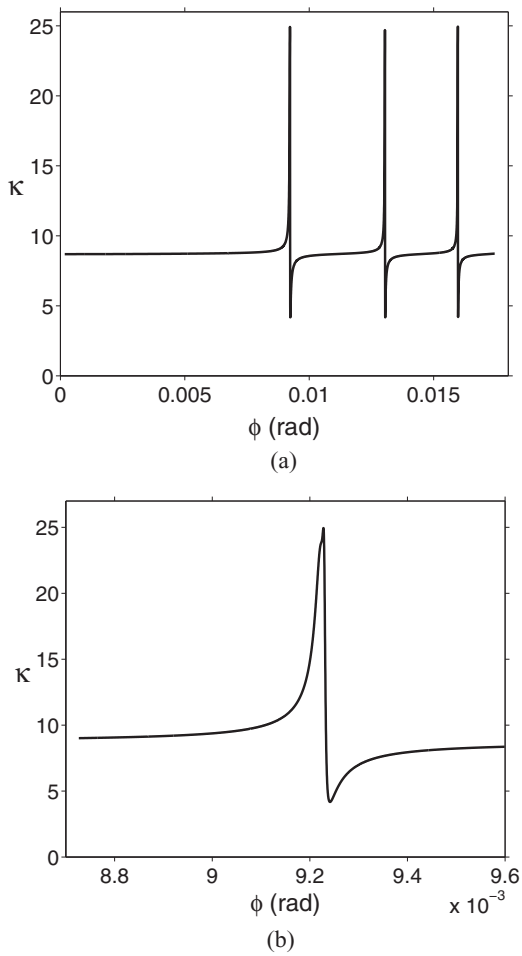

FIG. 6. (a) The azimuthal Schmidt number κ determined theoretically as a function of ϕ for the case $p = q = 0$ and $\alpha = 0.5$. (b) An expanded view of (a) near $\phi = 0.009$ rad, showing that there are no singularities.

as the LG basis, but with a fixed radial dependence, leaving only the azimuthal index as the degree of freedom. In such a case, the number of observed entangled modes is less than in the full down-converted state. The azimuthal Schmidt number quantifies this restricted number of observed modes.

We computed general expressions for the spectrum of OAM modes for the down-converted state in the LG basis, using the thin-crystal approximation to obtain analytic results. These expressions are applicable for arbitrary radial and azimuthal indices. Using these results, we computed the azimuthal Schmidt number for various radial index combinations and found that the azimuthal Schmidt number increases drastically at particularly small values of the down-conversion angle. In the case where the radial indices are zero the azimuthal Schmidt number can increase by as much as 3 times the nominal value at collinear down-conversion. Depending on the experimental parameters (the ratio of the down-converted beam radii to the pump beam radius), the maximum in the azimuthal Schmidt number appears as a narrow sharp peak. In such cases an extremely accurate angular adjustment would be required to locate the peak in an experimental setup. While the experimental setup in [24] allowed accurate angular adjustment [27], the spiral bandwidth was measured at only a single angle, and the exact angle of operation is not known. Hence, while we are able to explain the drastic increase in the azimuthal Schmidt number that was observed in [24], we are unable to verify the specific details.

ACKNOWLEDGMENT

We would like to thank Dr. Jacquiline Romero from the University of Glasgow for the discussions regarding the details of their experiment.

APPENDIX

In the case of degenerate type I phase matching we have $|\mathbf{k}_\mathrm{p}| = 2|\mathbf{k}_{\mathrm{s,i}}| = \omega_p/c$. From this we can write for the signal and idler beams

$$k_{\mathrm{s,i}z} = \sqrt{\frac{k_p^2}{4} - |\mathbf{q}_{\mathrm{s,i}}|^2} = \sqrt{\frac{k_p^2}{4} - \frac{k_p^2 \sin^2\phi}{4} - \left(|\mathbf{q}_{\mathrm{s,i}}|^2 - \frac{k_p^2 \sin^2\phi}{4}\right)}. \quad \text{(A1)}$$

The term

$$|\mathbf{q}_{\mathrm{s,i}}|^2 - \frac{k_p^2 \sin^2\alpha}{4} \quad \text{(A2)}$$

is small in the paraxial limit, so Eq. (A1) can be approximated as

$$k_{\mathrm{s,i}z} \approx \frac{k_p \cos\phi}{2} - \frac{|\mathbf{q}_{\mathrm{s,i}}|^2 - \frac{1}{4}k_p^2 \sin^2\phi}{k_p \cos\phi}. \quad \text{(A3)}$$

In the paraxial limit $k_{\mathrm{p}z}$ can be written as

$$k_{\mathrm{p}z} = \sqrt{k_\mathrm{p}^2 - |\mathbf{q}_\mathrm{p}|^2} \approx k_\mathrm{p} - \frac{|\mathbf{q}_\mathrm{p}|^2}{2k_p}. \quad \text{(A4)}$$

Finally, by using Eqs. (6) and (7) we obtain

$$\Delta k_z = n_\mathrm{o}\left[\frac{\lambda_\mathrm{p}|\mathbf{q}_\mathrm{i} - \mathbf{q}_\mathrm{s}|^2}{4\pi\cos(\phi)} - \frac{\pi\sin^2(\phi)}{\lambda_\mathrm{p}\cos(\phi)}\right]. \quad \text{(A5)}$$

[1] M. A. Nielsen and I. L. Chuang, *Quantum Computation and Quantum Information* (Cambridge University Press, New York, 2010).
[2] A. Mair, A. Vaziri, G. Weihs, and A. Zeilinger, Nature (London) **412**, 313 (2001).
[3] S. Franke-Arnold, S. M. Barnett, M. J. Padgett, and L. Allen, Phys. Rev. A **65**, 033823 (2002).
[4] J. P. Torres, A. Alexandrescu, and L. Torner, Phys. Rev. A **68**, 050301 (2003).
[5] H. Huang and J. H. Eberly, J. Mod. Opt. **40**, 915 (1993).
[6] C. K. Law, I. A. Walmsley, and J. H. Eberly, Phys. Rev. Lett. **84**, 5304 (2000).
[7] P. G. Kwiat, A. M. Steinberg, and R. Y. Chiao, Phys. Rev. A **47**, R2472 (1993).

[8] J. Brendel, N. Gisin, W. Tittel, and H. Zbinden, Phys. Rev. Lett. **82**, 2594 (1999).
[9] A. Aiello, S. S. R. Oemrawsingh, E. R. Eliel, and J. P. Woerdman, Phys. Rev. A **72**, 052114 (2005).
[10] B. Jack, A. M. Yao, J. Leach, J. Romero, S. Franke-Arnold, D. G. Ireland, S. M. Barnett, and M. J. Padgett, Phys. Rev. A **81**, 043844 (2010).
[11] J. Leach, B. Jack, J. Romero, A. Jha, A. M. Yao, S. Franke-Arnold, D. G. Ireland, R. W. Boyd, S. M. Barnett, and M. J. Padgett, Science **329**, 662 (2010).
[12] J. G. Rarity and P. R. Tapster, Phys. Rev. Lett. **64**, 2495 (1990).
[13] D. Bouwmeester, J. W. Pan, K. Mattle, M. Eible, H. Weinfurter, and A. Zeilinger, Nature (London) **390**, 575 (1997).
[14] D. Boschi, S. Branca, F. DeMartini, L. Hardy, and S. Popescu, Phys. Rev. Lett. **80**, 1121 (1998).
[15] X. S. Ma, T. Herbst, T. Scheidl, D. Wang, S. Kropatschek, W. Naylor, B. Wittmann, A. Mech, J. Kofler, E. Anisimova *et al.*, Nature (London) **489**, 269 (2012).
[16] A. Ekert and P. Knight, Am. J. Phys. **63**, 415 (1995).
[17] C. K. Law and J. H. Eberly, Phys. Rev. Lett. **92**, 127903 (2004).
[18] G. Molina-Terriza, J. P. Torres, and L. Torner, Phys. Rev. Lett. **88**, 013601 (2001).
[19] B. J. Pors, C. H. Monken, E. R. Eliel, and J. P. Woerdman, Opt. Express **19**, 6671 (2011).
[20] F. M. Miatto, A. M. Yao, and S. M. Barnett, Phys. Rev. A **83**, 033816 (2011).
[21] F. M. Miatto, D. Giovannini, J. Romero, S. Franke-Arnold, S. M. Barnett, and M. J. Padgett, Eur. Phys. J. D **66**, 1 (2012).
[22] M. P. van Exter, A. Aiello, S. S. R. Oemrawsingh, G. Nienhuis, and J. P. Woerdman, Phys. Rev. A **74**, 012309 (2006).
[23] H. Di Lorenzo Pires, H. C. B. Florijn, and M. P. van Exter, Phys. Rev. Lett. **104**, 020505 (2010).
[24] J. Romero, D. Giovannini, S. Franke-Arnold, S. M. Barnett, and M. J. Padgett, Phys. Rev. A **86**, 012334 (2012).
[25] B. E. A. Saleh, A. F. Abouraddy, A. V. Sergienko, and M. C. Teich, Phys. Rev. A **62**, 043816 (2000).
[26] F. S. Roux, Phys. Rev. A **83**, 053822 (2011).
[27] J. Romero (private communication).